

## Solar radiation and ambient temperature effects on the performances of a PV pumping system

N. Hamrouni\*, M. Jraidi and A. Chérif

Electrical Systems Laboratory,  
High Engineering Faculty of Tunis, P.B. 37, 1002 Le Belvedere, Tunis, Tunisia

(reçu le 26 Janvier 2008 – accepté le 30 Mars 2008)

**Abstract** - This paper presents the influence of the solar radiation and ambient temperature variation on the performance of a stand alone photovoltaic pumping system which composed of a PV generator, DC-DC adaptor, DC-AC inverter and an immersed group motor-pump. Those performances such PV efficiency, inverter efficiency and flow rate are improved by a judicious control implanted on the converters. The maximal power point tracking (MPPT) control allows the extraction of the maximum output power delivered by the PV generator. However the inverter insures a pulse width modulation (PWM) control of the asynchronous motor and a sine wave form of output signals. We proceed to modelling the PV pumping system with power electronic converters allowing respectively optimal operating point tracking and power conversion under the appropriate command. From the obtained simulation results, under Matlab/Simulink environment, we will discuss how the ambient temperature and the solar radiation influence the performance of the PV plants. The experimental results of the PV pumping system installed in Tunisia (2.1 kWc) verify the validity of the model and the proposed controller.

**Résumé** - Cet article présente l'influence de l'irradiation solaire et de la variation de la température ambiante sur les performances d'un système de pompage photovoltaïque composé d'un générateur photovoltaïque, d'un adaptateur DC-DC, d'un onduleur DC-AC et d'un groupe moteur-pompe immergé. Ces performances telles que le rendement photovoltaïque, le rendement de l'onduleur et le taux du débit, sont améliorées par un système de contrôle judicieux implanté sur les convertisseurs. Le système de contrôleur du point de puissance maximale (MPPT) permet l'extraction du maximum de la puissance de sortie délivrée par le générateur photovoltaïque. Mais l'onduleur assure le contrôle de la modulation de largeur d'impulsions (PWM) du moteur asynchrone et de la forme de l'onde sinusoïdale des signaux de sortie. Nous procédons à la modélisation du système de pompage photovoltaïque avec des convertisseurs électroniques de puissance permettant de suivre respectivement le point optimal de fonctionnement et le rendement de conversion dans le cadre de la commande appropriée. A partir des résultats de simulation obtenus dans l'environnement Matlab/Simulink, nous allons discuter de l'influence de la température ambiante et du rayonnement solaire sur le fonctionnement des centrales photovoltaïques. Les résultats expérimentaux du système de pompage photovoltaïque installé en Tunisie (2,1 kWc) permettent de vérifier la validité du modèle et du contrôleur proposé.

**Key words:** Irradiance - Modelling - Control - Temperature - Pumping system.

### 1. INTRODUCTION

Right from the beginning the photovoltaic solar power represents one of the most promising renewable energy in the world. Among of its advantages, two main obstacles for using solar energy are the high initial costs and the very low PV cell conversion efficiency. The use of photovoltaic as the power source for pumping water is considered as one of the most promising areas of PV application. Photovoltaic water pumping systems are particularly suitable for water supply in remote areas where no electricity supply is available. Water can be pumped during the day and stored in tanks, making water available at night or when it is cloudy. The pumped water can be used in many applications such as domestic use, water for irrigation and village water supplies. The advantages of using water pumps powered by photovoltaic systems include low

---

\* Hamrouni\_nejib2003@yahoo.fr

maintenance, ease of installation, reliability and the matching between the powers generated and the water usage needs. In addition, water tanks can be used instead of batteries in photovoltaic pumping systems.

The efficiency of the PV pumping system depends on several climatic factors such as the solar radiation, the ambient temperature and the state of the solar panels (ageing, cleanliness...) [1]. Photovoltaic powered water pumping systems require only that there be adequate sunshine and a source of water. The use of photovoltaic power for water pumping is appropriate, as there is often a natural relationship between the availability of solar power and the water requirement. Water requirement increases during hot weather periods when the solar radiation intensity is high and the output of the solar array is at its maximum. On the other hand, the water requirement decreases when the weather is cool and the sunlight is less intense [2]. The DC power generated by the PV modules is linearly dependent on the irradiance, except for small values of irradiance when the output power is zero. The efficiency of the PV plant is not only strongly depends on irradiance but also depends on the module temperature [3].

Since the maximum power point varies with radiation and temperature, it is difficult to maintain optimum matching at all radiation levels. In order to improve the performance of a PV pumping system, a DC-DC converter known as a maximum power point tracker (MPPT) is used to match continuously the solar cell power to the environment changes. Many algorithms have been developed for tracking the maximum power [10]. The main objective of this work is to study the influence of the irradiance and the ambient temperature on the global efficiency and consequently on the water flow generated by the pump. A computer program is developed for each component to simulate the performance of the different components of the PV pumping system which composed of PV generator, DC-DC adaptor, DC-AC inverter and an immersed motor-pump.

In the first part a complete model [4] simulating the above architecture of the PV pumping system is done on Matlab/Simulink environment. After, we will study the effect of the solar radiation and the ambient temperature variations on the performances of the stand alone PV pumping system. In the last part we will illustrate some typical variation of a reel pumping system installed in Louata - Tunisia, in order to evaluate our obtained simulation results.

## 2. DESCRIBING AND MODELLING OF PV PUMPING SYSTEM

The typical configuration of the PV pumping system is shown in Fig 1. It is composed of a PV generator, a power DC-DC adapter, a natural sinusoidal PWM voltage source inverter and a three phase squirrel cage induction motor driving a centrifugal pump.

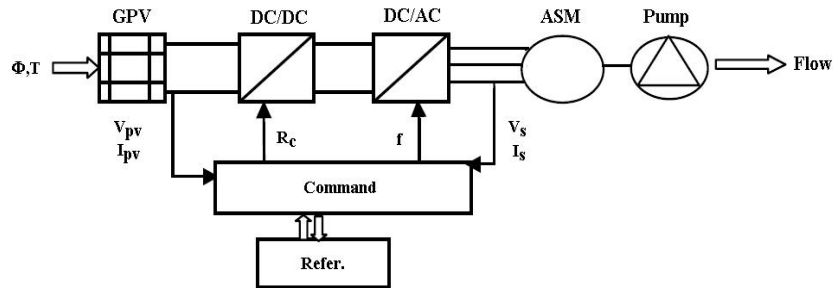


Fig. 1: General block diagram of the PV pumping system

### 2.1 Photovoltaic Generator

The photovoltaic generator is neither a constant voltage source nor a current source. It is modelled and described by the relation between current and tension [4].

$$I_{pv} = I_{ph} - I_s \left[ \exp\left(\frac{q}{n k T}\right) \cdot (V_{pv} + I_{pv} \cdot R_s) - 1 \right] - \left( \frac{1}{R_{sh}} \right) \cdot (V_{pv} + I_{pv} \cdot R_s) \quad (1)$$

where:

$$T = T_a + k_t \cdot \Phi, \quad I_{ph} = (I_{sc} + T_{coef}(T - T_{offs})) \cdot \Phi / 1000,$$

$$I_s = I_{s0} T^3 \times \exp(-e \cdot U_{gap} / k \cdot T), \quad A = e / (n \cdot k \cdot T)$$

$$k = 1.38066 \cdot 10^{-23} \text{ J/K}, \quad q = -1.602189 \cdot 10^{-19} \text{ C}.$$

The solar cells are connected in a series- parallel configuration to match the required solar voltage and power rating. The mathematical equation for the array current and voltage becomes as follows:

$$I_{pvg} = N_p \times I_{ph} - N_p \times I_s \cdot \left[ \exp \left[ \left( \frac{q}{n \cdot k \cdot T} \right) \cdot \left( \frac{V_{pv} + I_{pv} \cdot R_s}{N_s} + \frac{I_{pv} \cdot R_s}{N_p} \right) \right] - 1 \right] - \frac{N_p}{R_{sh}} \cdot \left( \frac{V_{pv} + I_{pv} \cdot R_s}{N_s} + \frac{I_{pv} \cdot R_s}{N_p} \right) \quad (2)$$

where  $N_p$  is the number of the parallel modules and each module is composed of  $N_s$  cells connected in series. For standard climatic conditions (1000 W/m<sup>2</sup>, 25 °C), the simulated I-V characteristic for a photovoltaic module formed by crystal mono silicon cells (40 series cells), is presented by the figure 3. The models parameters are calculated experimentally for an AEG PC4050 type PV module [5].

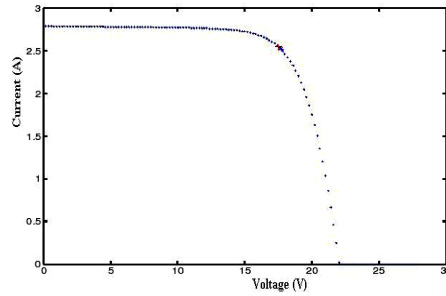


Fig. 2: Simulated I-V characteristic of a PV module

## 2.2 Back Boost Chopper

The back boost chopper is inserted between the solar generator and the load. Its duty cycle  $\alpha$  ( $0 < \alpha < 1$ ) linked to the ratio between the input and the output voltage when the conduction is continued by the relationship:  $V_s = \alpha V_e$  (losses are neglected).

## 2.3 Inverter

The inverter provides three-phase system voltages variable in amplitude and frequency to operate with variable loads and frequency (from 0.1 up to 1 time the rated frequency) [5]. The current is modulated sinusoidally to obtain a high efficiency. The pulse frequency is equal to 2 kHz.

The phase voltage can be expressed as the example below [6]:

$$\begin{bmatrix} v_{as} \\ v_{bs} \\ v_{cs} \end{bmatrix} = \frac{\alpha V_{pv}}{3} \begin{bmatrix} 2 & -1 & -1 \\ -1 & 2 & -1 \\ -1 & -1 & 2 \end{bmatrix} \cdot \begin{bmatrix} c_1 \\ c_2 \\ c_3 \end{bmatrix} \quad (3)$$

with  $\alpha V_{pv}$  is the input voltage.  $c_1$ ,  $c_2$  and  $c_3$  are the PWM control signals.

The harmonics which appear as sidebands centred on the switching frequency are naturally filtered by the motor itself.

### 2.4 The asynchronous motor 'ASM'

To modulate the ASM, we have selected the phase model. It is defined by the equations of stator and rotor voltages, the magnetic flux, the electromagnetic torque and the mechanical equation [7]. The diagram of the corresponding model developed on Matlab/Simulink is given by the figure 3.

Where:

$$a_{11} = a_{22} = \frac{1}{\sigma l_s}, \quad a_{11} = a_{22} = \frac{1}{\sigma l_r}, \quad a_{31} = a_{41} = a_{14} = a_{24} = \frac{2}{\sqrt{3}} \frac{M}{\sigma l_r l_s},$$

$$a_{32} = a_{42} = a_{13} = a_{23} = -\frac{2}{\sqrt{3}} \frac{M}{\sigma l_r l_s}, \quad \sigma = 1 - \frac{M^2}{l_r l_s}.$$

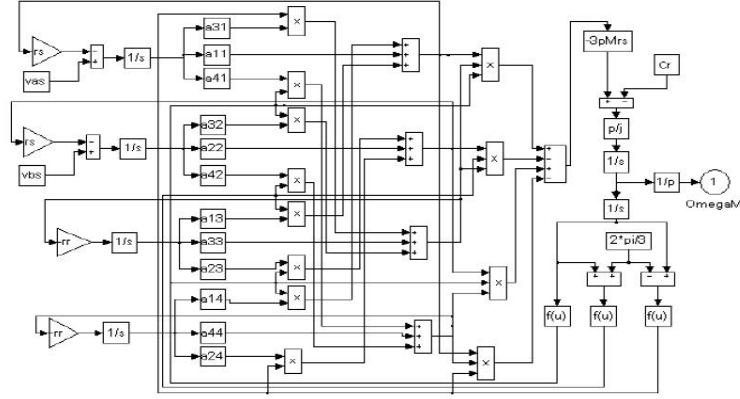


Fig. 3: Simulink model diagram of the ASM

### 2.5. The pump [8]

The centrifugal pump load torque  $C_r$  is assumed to be proportional to the square of the rotor speed.

$$C_r = k \left( 1 - \frac{\omega_r}{\omega_s} \right)^2 \cdot \omega_s^2 \quad (4)$$

$k$  is a constant and depends on pump nominal data.

The flow head characteristic of a centrifugal pump is given by the following expression:

$$H_n = a_1 \cdot \omega^2 + a_2 \cdot \omega \cdot Q + a_3 \cdot Q^2 \quad (5)$$

The motor speed is expressed as follow:

$$\omega = \left( 1 - \frac{\omega_r}{\omega_s} \right) \cdot \omega_s \quad (6)$$

The pump efficiency is defined as the ratio of the hydraulic power imparted by the pump to the fluid to the shaft mechanical power. It is expressed by the following equation:

$$\eta = \frac{\bar{w} \cdot Q \cdot H_n}{k \cdot \left( 1 - \frac{\omega_r}{\omega_s} \right)^3 \cdot \omega_s^3} \quad (7)$$

Based on the preceding expressions we developed the diagram of the pump model on Matlab/Simulink environment which is shown in figure 4.

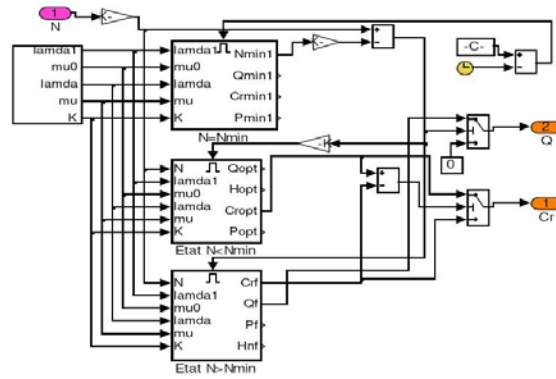


Fig. 4: Pump scheme structure

The figure 5 represents the different characteristics of the flow rate and the load torque of the pump. The simulated responses of flow and torque versus the motor speed have shown for our functioning point corresponding to a speed of 3000 rd/min. For  $N = 3000$  rd/min, the optimal pump flow is about  $2.3 \text{ m}^3/\text{h}$  whereas the resistant torque is about  $5.4 \text{ N.m}$ .

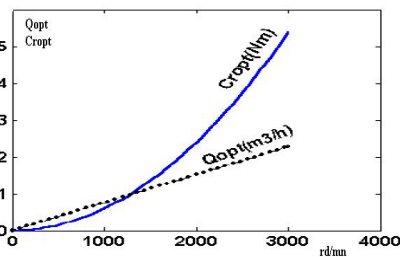


Fig. 5: Flow rate and load torque curves of the pump versus the motor speed

### 3. CONTROL

The figure 6 shows the basic elements of the PV pumping system and control loop block implemented in Matlab/Simulink diagram. The main system components are: photovoltaic array to provide electricity, DC-DC converter, DC-AC inverter, asynchronous machine, pump, maximum power point tracking (MPPT) and V/f command.

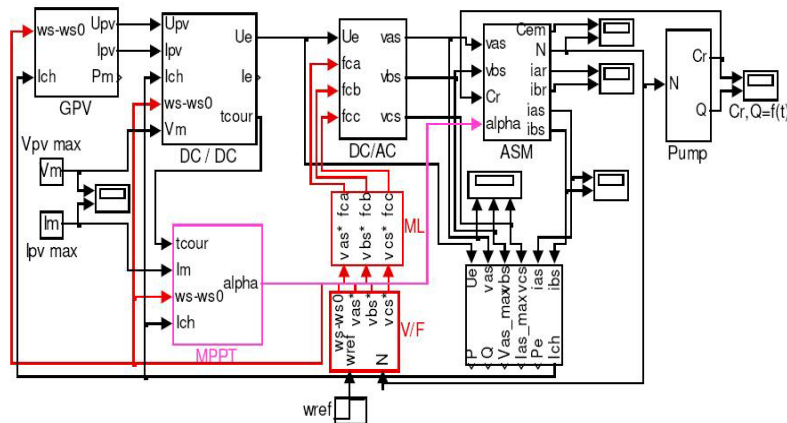


Fig. 6: Simulink program of PV pumping system

**3.1 Maximal power point tracking law (MPPT)**

The DC/DC converter should always operate in the maximum power point tracking to maximize the PV generator efficiency and consequently increase the efficiency of the global system. The optimum power of PV generator fluctuates instantaneously with the climatic conditions (solar flow, temperature and wind speed). The coupling of a load at constant power, without using of the battery, does not ensure an optimal operation. It is then essential to envisage an adapter of impedance making it possible the responsibility of extract the maximum power from PV generator.

This technique of MPPT was applied by different ways and means [9]. By using an intelligent algorithm, it ensures the PV module always operates at its maximum power point as the temperature, insulation and load vary. A number of tracking algorithms [10] have been proven and used and a number of DC/DC converter topologies are possible. In this study, we execute this technique with the use of an intelligent algorithm.

It consists to research the real operation point of the load  $P_{ch}$  (before adaptation) and to deduce the dynamic factor for adaptation ( $\alpha$ ) as being the relationship between the maximum power from PV generator and  $P_{ch}$ . By action using this factor, we will be able to adapt the load to the maximum power provided by PV generator. The MPPT algorithm used is represented by the following diagram.

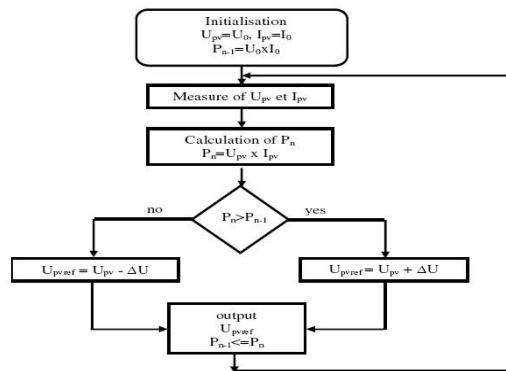


Fig. 7: Schematic diagram of the MPPT command of the DC-DC converter

**3.2 The V/f law**

We distinguish two essential controls laws which are the vectorial control and the V/f command. V/f control will be best adopted for this system [11]. A schematic diagram of the V/f command used for our study is presented in figure 8.

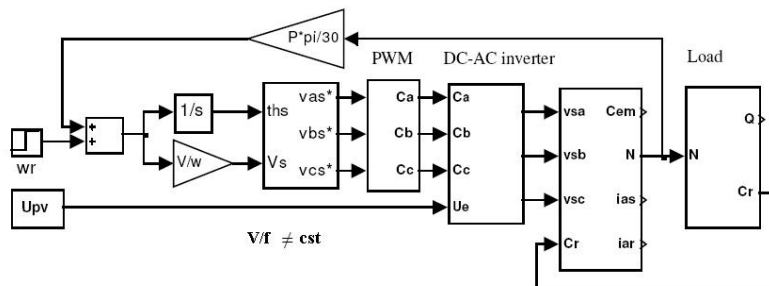


Fig. 8: Schematic diagram of the V/f command of the DC-AC inverter

Because the DC link voltage varies with the climatic conditions, the traditional  $V/f$  command will not be constant but will vary with the time to ensure a maximal PV pumping operation during the day. The relation of the output voltage at the  $V/f$  frequency can be regulated in a constant or variable way, according to requirements of drive, function of the frequency, of the disturbances, of the load and of the climatic conditions (Weak solar flow). For example, for lower radiations, after 15 h 00 PM, the inverter frequency decreases to  $(40 \pm 10)$  Hz. At the moment of starting, the  $V/f$  ratio is lifted for a short period, which results in a high starting moment [12].

This idea was explained by a diagram representing the variation of the  $V/f$  ratio versus the solar radiation for the PV pumping system, investigated in this paper.

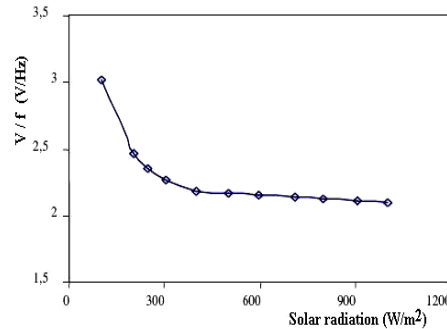


Fig. 9:  $V/f$  ratio versus the solar radiation

#### 4. SIMULATION AND RESULTS

The simulated results obtained with the Simulink tool integrated the MPPT command and the  $V/f$  laws are in the steady state operation mode. The system is composed of a PV generator (230 V/ 2100 W<sub>p</sub>), an MPPT power adapter, a three phase inverter (3 kVA/12...127 V/5...60 Hz) and a submersed motor-pump group (1.5 kW / 3 x 127 V/ 50 Hz). All these components form the association is shown in the figure 1. The PV generator is composed of 3 parallel and 14 series modules. Those modules are polycrystalline. Each module is formed by 40 series cells.

##### 4.1 Influence of the temperature variation [13]

As known, meteorological parameters, especially the array temperature do not remain constant all day long, but change considerably. It is then worth investigating the influence of the daily average temperature variation on the performances of the optimized system. For several temperature data between 5 and 75 °C and constant solar radiation equal to 1000 W/m<sup>2</sup>, we have presented the characteristic  $I_{pv} = f(V_{pv})$  of PV generator, the variations versus the temperature of the inverter frequency, the pump flow  $Q$  and the global efficiency of the PV system are illustrated in the figure 10.

Figure 10 display the simulation results as a function of temperature, obtained for a constant solar radiation equal to 1000 W/m<sup>2</sup>. The increase of the temperature yields a significant decrease of the inverter frequency and therefore the pump flow rate. As a result, the global PV system efficiency decreases about 0.03 %/°C. The open circuit voltage decreases as the temperature increases.

The increase of the PV power as a consequence of the temperature decreases leads to an improvement of the flow rate and, then, to an elevation of the daily water amount. It has been concluded these performances are degraded once the temperature increases. As a result the sizing of the system should be done in accordance with the average daily temperature of the site.

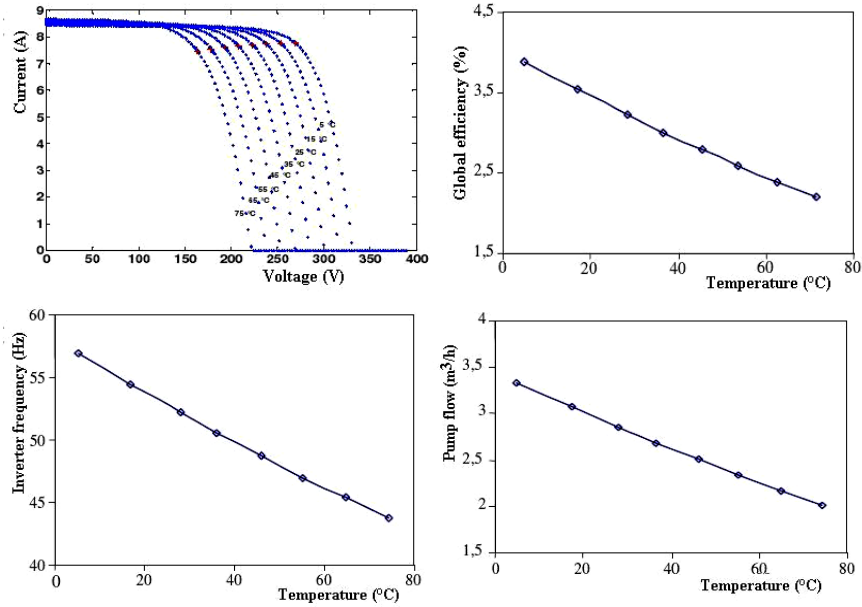


Fig. 10: PV system characteristics versus the ambient temperature at constant solar radiation

**4.2 Influence of the solar radiation changing**

For several solar radiation varies between 100 to 1000 W/m<sup>2</sup> and for a constant temperature equal to 25 °C, we have presented the characteristic  $I_{pv} = f(V_{pv})$  of PV generator, the variations versus the solar radiation of the maximal output PV generator power, the inverter frequency, the pump flow and the global efficiency of the PV system.

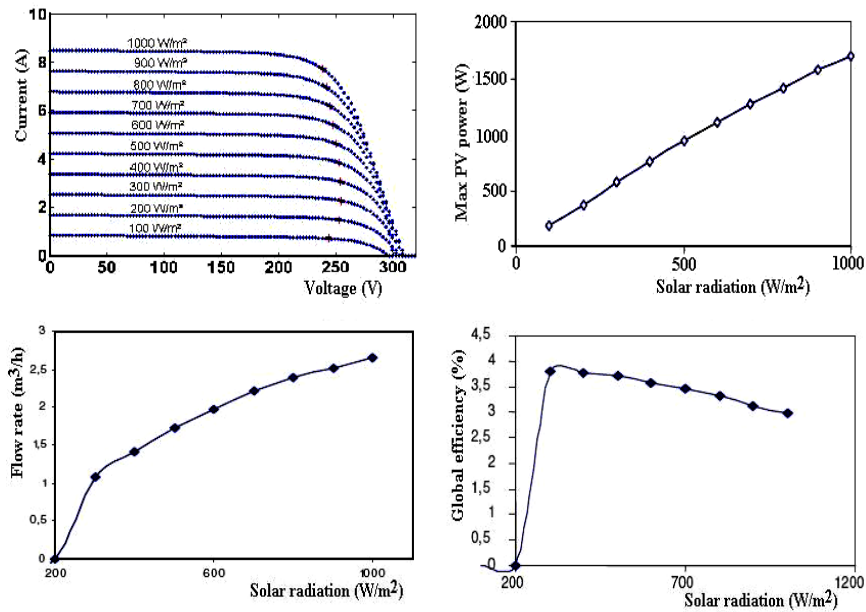


Fig. 11: PV system characteristics versus the solar radiation at constant ambient temperature

Figure 11 shows the obtained simulation results versus the solar radiation at constant temperature equal to 25 °C. The PV generator power increases as the solar radiation increases, and therefore the pump flow rate. As a result, the global PV system efficiency increases and still constant equal to 3 %. The short circuit current increases linearly with the radiation level.

#### 4.3 Normal Mode

For different couple of solar radiation and ambient temperature during a normal day, we recorded the simulation results versus the time of the pump flow rate, the maximum power provided by the PV generator, the inverter frequency and the total efficiency of the PV pumping system.

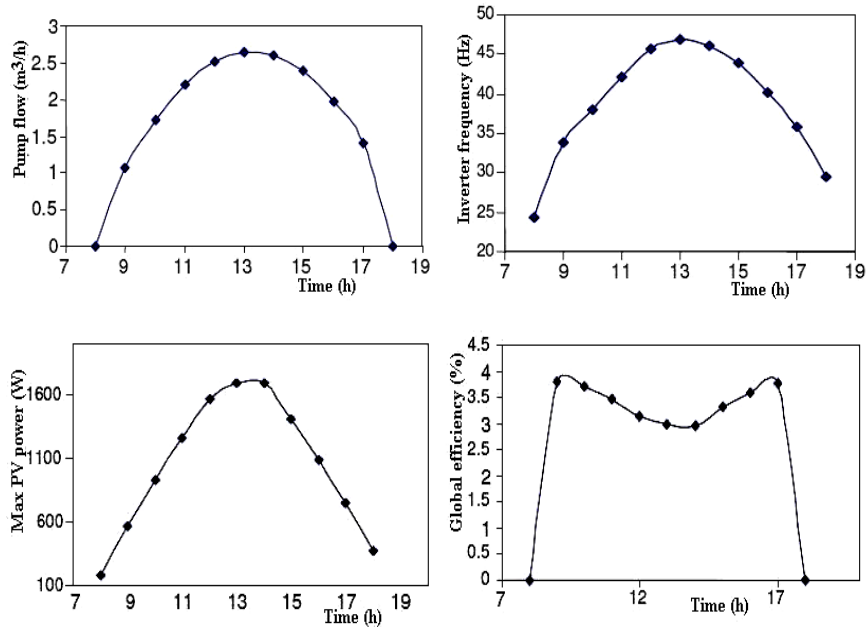


Fig. 12: PV system characteristics versus the solar radiation and ambient temperature during a normal day

The pump provided the water for a maximum PV power equal to 200 W/m<sup>2</sup> obtained for 25 Hz inverter frequency. As a result, the global PV system efficiency still constant equal to 3 %. The maximum of the pump flow (2.5 m<sup>3</sup>/h) is obtained at the mid day for 1600 W/m<sup>2</sup> PV generator.

#### 4.4 Disturbed Mode

For disturbance meteorological parameters; solar radiation and ambient temperature, we recorded the simulation results versus the time of the pump flow rate, the maximum power provided by the PV generator, the inverter frequency and the total efficiency of the PV pumping system.

For a transition of a cloud between 14 h 00 and 15 h 00 in the afternoon, we have presented the following figures.

For disturbance meteorological parameters; solar radiation and ambient temperature recorded in the afternoon, due to the transition of a cloud, these different characteristics of the PV pumping system are decreased. The maximum PV generator is decreased to 1000 W/m<sup>2</sup>, consequently the pump flow rate is decreased to 1.6 m<sup>3</sup>/h. The total efficiency of the PV system oscillates round 3 %.

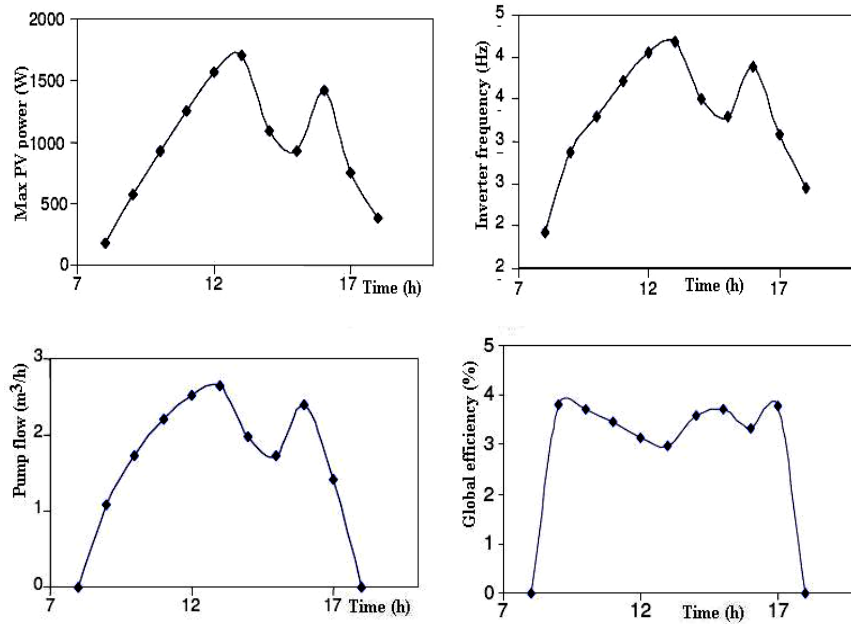


Fig. 13: PV system characteristics versus the solar radiation and ambient temperature for disturbance meteorological parameters

## 5. EXPERIMENTAL RESULTS

Within the frame of the German-Tunisian Cooperation for the promotion of renewable energies, 14 photovoltaic pumping systems (2.1 and 2.8 kW<sub>p</sub>) have been installed in Tunisia [14] in order to demonstrate the reliability of this technology and to evaluate the conditions for an economic competition. In fact it can contribute to the improvement of the water supply in rural regions of Tunisia.

These systems have been equipped by several data acquisition systems collecting meteorological data, well characteristics, pump 's flow rate and water consumption and allowing to identify the reason in case of unexpected stops. Among obtained results, we present the most important results for Louata PV pumping plant sets in Kairouan-Tunisia (Fig. 14).

Its principal Characteristics are:

PV power: 2.1 kW<sub>p</sub>

Total height: 65 m

Water demand: 2 m<sup>3</sup>/day

Global efficiency: 3 %

Necessary PV power: 1.7 kW

Pump flow (1000 W/m<sup>2</sup>): 2.5 m<sup>3</sup>/h

Hydraulic power (6.4 hours): 320 W

The collected data have been analysed and treated in order to evaluate the performances and the characteristic parameters of these systems and to interpret precisely their evolution opposite the typical using compartment. We have illustrated by the following figures the typical variations of the Louata PV pumping system, in order to validate our developed models and commands investigate in the previously part.

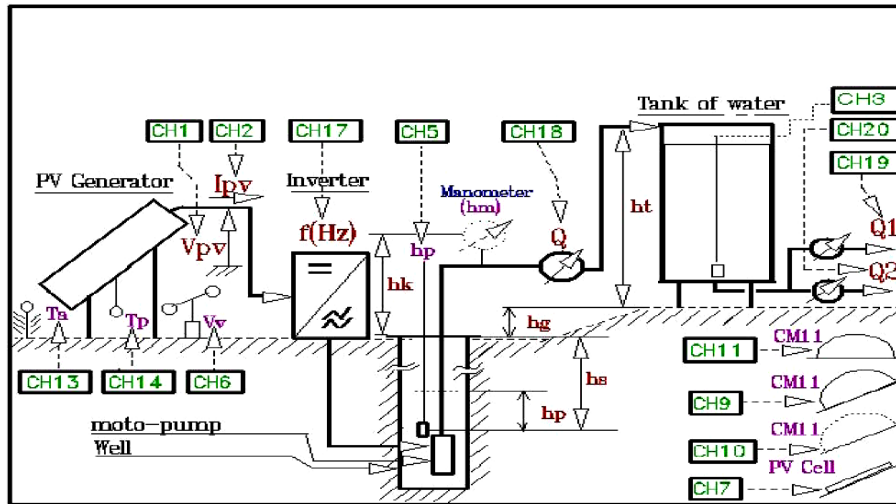


Fig. 14: Data acquisition system of a PV pumping plants in Tunisia

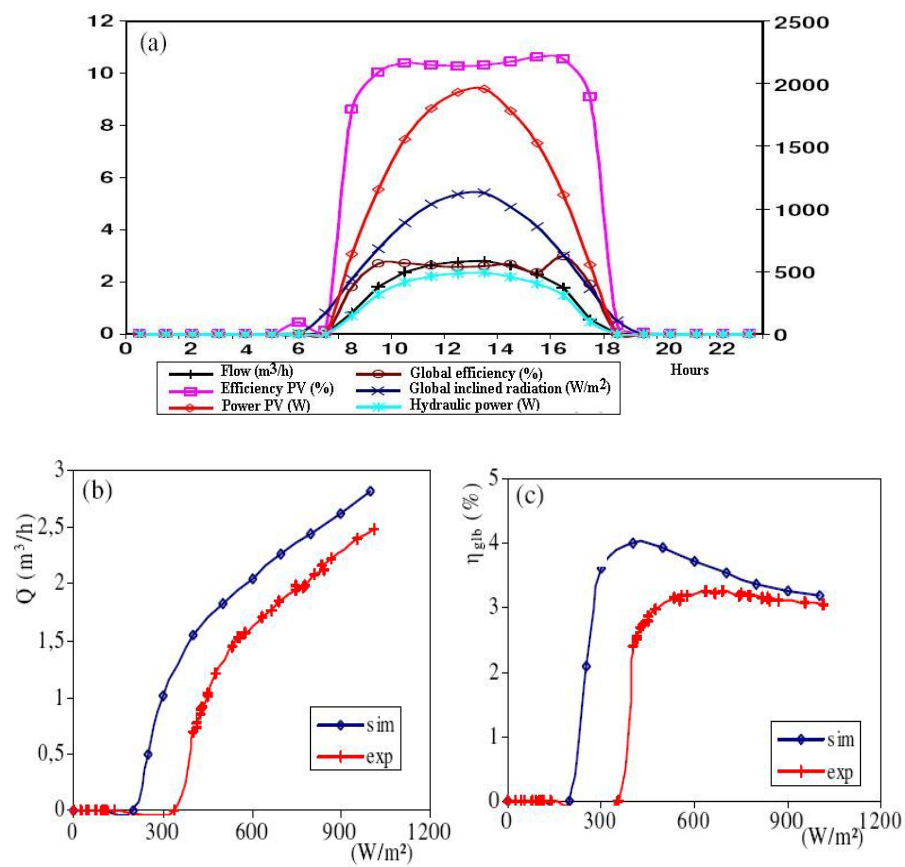


Fig. 15: Experimental and simulating results of a PV pumping system

Figure 15 shows the important characteristics of the experimental PV pumping system. The maximum of the pump flow ( $2.5 \text{ m}^3/\text{h}$ ), the global efficiency (3 %) and the PV power (1900W) are obtained in the midday (Fig. 15.a). For a constant ambient temperature ( $25^\circ\text{C}$ ), the optimal flow rate is obtained for irradiance equal to  $1000 \text{ W}/\text{m}^2$ , corresponding to a global efficiency equal to 3 % (Fig. 15.b and c). As a result of the comparison between the experimental and the simulation, we can conclude that there is a similarity and concordance.

## 6. CONCLUSION

The goal achieved via this study is the investigation of the influence of the ambient temperature and solar radiation changing effects on the system performances. The obtained simulation results show that for large ambient temperature a decrease of the pump flow and the global efficiency, however a large solar radiation increase both the global efficiency and the pump flow.

It has been concluded that these performances are maximal in the midday, but are degraded when the meteorological parameters disturb. In the last part of the paper, we have present several results of an experimental PV pumping system for a normal day. For normal functioning mode, all figures show a good concordance and similarity between the experimental and the simulated system.

## REFERENCES

- [1] Il-Song Kim, 'Robust Maximum Power Point Tracker Using Sliding Mode Controller for Three-Phase Grid-Connected Photovoltaic System', *Solar Energy*, Vol. 81, N°3, pp. 405 – 414, 2007.
- [2] A.A. Ghoneim, 'Design Optimization of Photovoltaic Powered Water Pumping Systems', *Energy Conversion and Management*, Vol. 47, N°11-12, pp. 1449 – 1463, 2006.
- [3] S. Chokmaviroj, R. Wattanapong and Y. Suchart, 'Performance of a 500 kWp Grid Connected Photovoltaic System at Mae Hong Son Province, Thailand', *Renewable Energy*, Vol. 31, N°1, pp. 19 – 28, 2006.
- [4] M. Jraidi, 'Modélisation et Commande d'un Système de Pompage Photovoltaïque', Thèse de Doctorat, ENIT, 2005.
- [5] M. Jraidi, N. Hamrouni, A. Chérif et A. Dhoub, 'Modélisation et Simulation des Systèmes de Pompage Photovoltaïque avec de Nouvelles Stratégies de Commande', *JTEA'2004*, Hammamet, Tunisie, 2004.
- [6] G. Séguier, '*Les Convertisseurs de l'Electronique de Puissance, la Conversion Continu – alternatif*', Tome 4, Technique et Documentation, Lavoisier, France, 1987.
- [7] N. Hamrouni, M. Jraidi, A. Chérif and A. Dhoub, 'Modelling, Simulation and Control of PV Pumping System', *Electrimacs'05*, Hammamet, Tunisia, 2005.
- [8] Zhu Zuhcao, 'Theoretical Study and Engineering Implementation Superlow-Specific-Speed High Speed', *Ji Xie Gong Cheng Xue Bao (Journal of Mechanical engineering)*, Vol. 36, N°4, pp. 30 – 33, 2000.
- [9] A. Saadi et A. Moussi, 'Etude de l'Effet des Fluctuations de Température sur les Techniques d'Optimisation des Systèmes de Pompage Photovoltaïque', *CEE'2002*, Batna, Algeria, pp. 232 - 237, Octobre 2002.
- [10] M. Veerachary and N. Yadaiah, 'ANN Based Peak Power Tracking For PV Supplied DC Motors', *Solar Energy*, Vol. 69, N°4, pp. 343 – 350, 2000.
- [11] C.M. Liaw and C.W. Tsong, 'High Performance Speed Controller for Voltage Source Inverter Fed Induction Motor Drives', *IEEE Proceedings-b*, Vol. 139, N°3, May 1992.
- [12] Document, 'SPTP 42-3/42-30 of Bouaissi Plant, Exploitation Manual of PV Pumping Project in Tunisia', Deutsche Aerospace AG, 1994.
- [13] A. Betka and A. Moussi, 'Cell Temperature and Head Effects on the Performances of a Direct Photovoltaic Pumping System Driven by an Induction Motor', *Rev. Energ. Ren., ICPWE*, pp. 47 – 52, 2003.
- [14] A. Ounali, 'Projet de Démonstration de 14 Pompes Photovoltaïques', Agence pour la Maîtrise de l'Energie, Tunis 1996.